An Experimental Study on the Unsteady Extinction Limit Extension of a Counter-flow Diffusion Flame Affected by Velocity Change

Uen Do Lee[1], Kwang Chul Oh[1], Ki Ho Lee[2], Eui Ju Lee[3] & Hyun Dong Shin [1]

[1] Department of Mechanical Engineering, KAIST, Korea
[2] Research & Development Division for Hyundai Motor Company, Korea
[3] Department of Fire & Engineering Service Research Korea Institute of Construction Technology, Korea

Keywords: Unsteady extinction process, Extinction limit extension, Rayleigh Scattering, OH LIF

Abstract: Opposed jet diffusion flames affected by velocity change were investigated to know why unsteady flames survive at higher strain rates that are much larger than the steady extinction limit. Time-dependent maximum flame temperature (T_{max}) and OH radical (Y_{OH}) were measured over time using Rayleigh scattering method and OH laser-induced fluorescence (LIF) respectively. In this experiment, unsteady extinction limits are much higher than the steady extinction limits and values of the T_{max} and $Y_{OH,max}$ near the unsteady extinction limit were much lower than those of the steady extinction. We found that both the unsteady response of the convective-diffusive zone and the diffusive-reactive zone affect to the extension of the unsteady extinction limit.

1. Introduction

Understandings of unsteady flames are important to the analysis of turbulent combustion and the study of laminar flames as well [1]. Various attempts have been made to understand the unsteady behavior of flames. Of these attempts, flame extinction has been a very useful experimental tool because the unsteady effect of a flame appears clearly near the extinction limit. By considering the characteristics of unsteady flow fields, we can classify previous studies into three categories: the study of flames under oscillating flow fields [2-4], the study of flames on evolving jets [5] and the study of flame-vortex interaction [7-10]. Generally, the unsteady interaction of the flame and flow can be divided into three sequential and overlapping zones: convection, diffusion, and reaction. Therefore, when a flame is affected by a velocity change, we should consider the unsteady behavior of each overlapping zone. The unsteady behavior of a convective-diffusive zone has been extensively discussed in other studies [2,7-10]. Recently, Santoro et al. examined the difference between steady extinction and vortex-induced extinction and they showed that the difference became modest when they subtracted the time lag of the convective-diffusive zone with the aid of the equivalent strain rate concept [7]. Kyritsis et al. measured the extinction scalar dissipation rate and they showed that the unsteady extinction limits are 5%~26% larger than the steady extinction limits [8]. Katta et al. and Oh et al. numerically investigated the interaction between flames and a vortex. They observed the unsteady extinction strain rates and scalar dissipation rates are extended as the velocity changes more rapidly. They discussed the time lag of the convective-diffusive zone and the diffusive-reactive zone [9,10]. Like this, the result that unsteady flames can survive at much severe flow conditions(higher strain rates or scalar dissipation rates) than a steady state have been reported in many studies. And many efforts have been performed to explain the extinction limit extension of the unsteady flames, however, this phenomena has not been fully understood yet [3,5,7-10].

In this study, we experimentally studied the extinction limit extension of unsteady counterflow flames affected by velocity change. To determine the unsteady behavior of a flame's convection, diffusion, and reaction zones, we measured the extinction limits of flames, the time-dependent flame temperature, and the OH radical of the unsteady extinction process. Using the equivalent strain rate concept we valued the unsteady effect of the convective-diffusive zone and we estimated the unsteady effect of the diffusive-reactive zone.

2. Experimental method

Figure 1 shows the experimental setup consists of three parts: a burner, a piston assembly, and a laser system for optical measurements. The burner was an opposed jet type. The main nozzle had an internal diameter of 14 mm; that of the co-flow nozzle was 20 mm, and the distance between the air and fuel nozzles was 14 mm. A quartz window for a laser beam was placed on the rear side of each burner for optical measurements. We supplied diluted fuel ($CH_4 + N_2$) to the right-hand main nozzle and dried air to the left and the same amount of N_2 to each co-flow nozzle. The piston assembly, composed of three pistons, was used to introduce changes in the velocities of the gas flow. The lower piston was an actuator and two upper pistons provided an equal velocity change for the air and fuel streams. The instantaneous velocity change at the

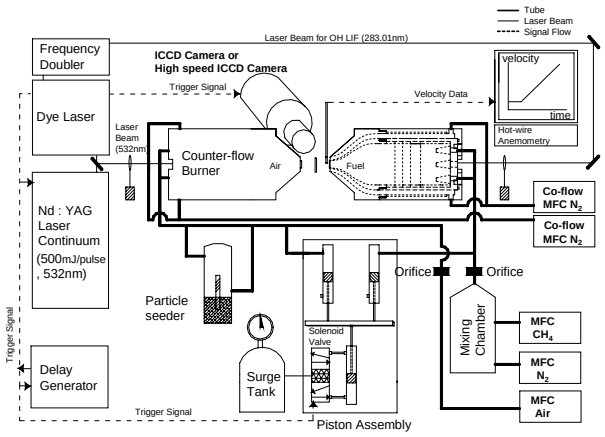

Fig. 1 Schematic of experimental

nozzle exit was measured by hot-wire anemometry.

We used two kinds of laser diagnostics for examining time-dependent temperature and OH radical in flames. The laser pulse for Rayleigh scattering was a second harmonic Nd:YAG laser (Continuum, 500 mJ, 532 ns) and an ICCD (Princeton Inc. 512 x 512) camera was used with a band pass filter (532nm, FWHM 10 nm). For OH radical measurements, using a dye laser and frequency doubler, the laser was tuned to 283.01 nm to excite the $Q_1 6$ line of the $A^2\sum^+ \leftarrow X^2\prod^+$ (v' = 1, v'' = 0) transition. An ICCD, with a UG-11 and a WG-305 filter, was used and the OH LIF measurement was conducted in the saturation regime. The transient chemi-luminescence images of the flame were taken with a high-speed ICCD (HICCD) camera (Phantom V7.0). The laser system, the ICCD camera, the HICCD camera, and the hot-wire anemometry were all synchronized with the piston movement by means of a pulse delay generator.

3. Results and Discussion

3.1. Unsteady Extinction Process

3.1.1. Change of flame luminosity. Figure 2 shows time-dependent evolutions of flame front during unsteady extinction process. The local quenching was observed after $\Delta t = 7$ ms. The flame quenching begins in the middle of the flame surface; as time passes, the quenching area evolves toward the axis and, subsequently, the flame of the inner region is eventually extinguished [6]. In this study, we defined the extinction point when the flame of the inner region eventually disappeared. For example, we determined that the eventual extinction occurred at $\Delta t = 15$ ms. During the whole process the initial position and shape of the flame were preserved. As such, we were able to measure the unsteady extinction limits. The strain rate was calculated using Eq.1 [11].

$$a = \frac{2(-V_{oxidant})}{L}\left(1+\frac{V_{fuel}}{(-V_{oxidant})}\left(\frac{\rho_{fuel}}{\rho_{oxidant}}\right)^{1/2}\right) \qquad (1)$$

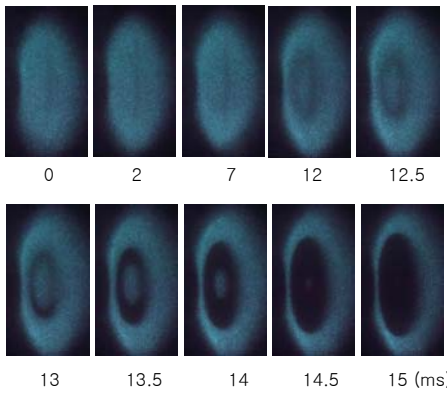

Fig. 2 Behavior of flame during the unsteady extinction process (CH_4:N_2= 5:5, $a_{initial}$ = 266.2 (1/s))

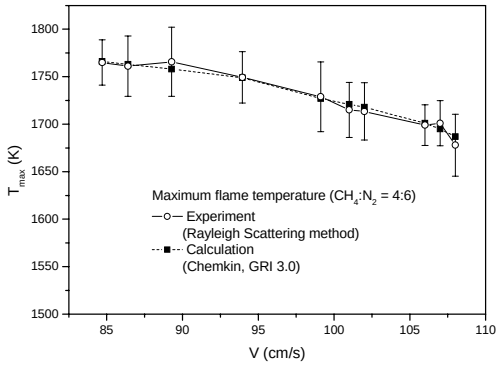

Fig. 3 Maximum flame temperature of steady flames with increasing velocity

3.1.2. Rayleigh Scattering Method. Figure 3 shows T_{max} from the Rayleigh scattering method and numerical calculation. T_{max} decreases as the velocity increases and the experimental results are similar to the numerical results. We can verify that the Rayleigh scattering method can be a good way of measuring the flame temperature without disturbing the flame. The Rayleigh scattering signal is proportional to the density and Rayleigh scattering cross section of molecular. Thus we can calculate the temperature by using the Rayleigh scattering signal of the ambient air ($R_{air,298K}$) and the Rayleigh scattering signal of the flame (R_{flame}) as Eq. 2 [12].

$$\frac{T_{flame}}{T_{air}} = \frac{(R_{air,298K} - R_{background\ noise})}{(R_{flame} - R_{background\ noise})} \cdot \frac{\left(\sum_i^n x_i \sigma_{Ri}\right)_{flame}}{\left(\sum_i^m x_i \sigma_{Ri}\right)_{air}} \qquad (2)$$

The mixture averaged Rayleigh cross-sections ($\sum x_i \sigma_{Ri}$) were obtained from numerical calculation [13,14]. The variations of Rayleigh cross section affect the estimation of T_{max} within 8 K of the entire experimental range.

3.1.3. Time-dependent Flame Temperature and OH radical. Figure 4 show the Rayleigh scattering signals

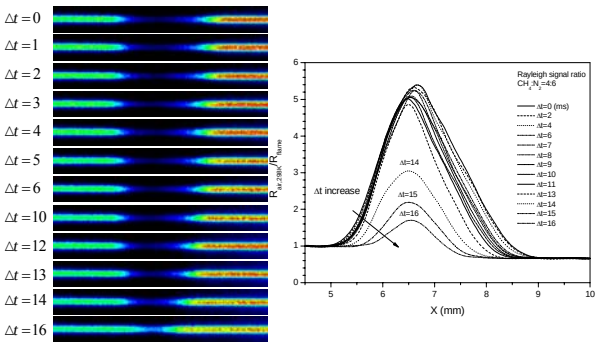

(a) (b)

Fig. 4 (a) Changes of the Rayleigh scattering signals over time (b) Signal ratio of the flame and ambient air (CH_4:N_2=4:6, $a_{initial}$ = 226.8 (1/s))

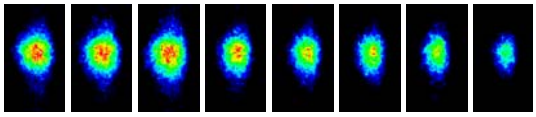

(a)

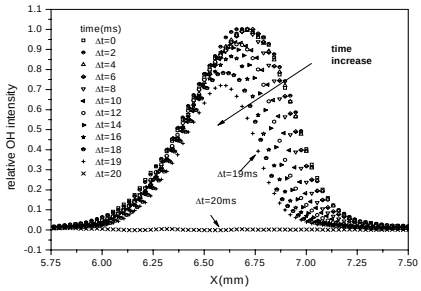

(b)

Fig. 5 (a) OH signal images over time (b) Distribution of OH LIF signals (CH_4:N_2= 5:5 $a_{initial}$ = 226.8 (1/s))

of unsteady extinction process. In Fig 4a, we can see the time-dependent change of the thermal layer qualitatively. Figure 4b shows the successive change of the signal ratios of the Rayleigh scattering and they can be transformed into the flame temperature profile with the proper consideration of the scattering cross section. Figure 5a shows time-dependent OH images of unsteady extinction process. The OH LIF signals show that the intensity and the distributed area of the OH radicals decrease over time. Figures 5b shows the one-dimensional profiles of the OH LIF intensities normalized by the OH peak of t = 0. The OH radical distributed in a narrow region (≈ 1 mm) comparing to the thermal layer shown in Fig. 4.

Figure 6 shows the strain rate change, steady and unsteady extinction points, and the time-dependent T_{max} and maximum OH intensity. Each unsteady extinction point was measured using chemi-luminescence images and it is much larger than the steady extinction point. T_{max} and OH radical is nearly constant in the starting region of the velocity change, then decreases gradually

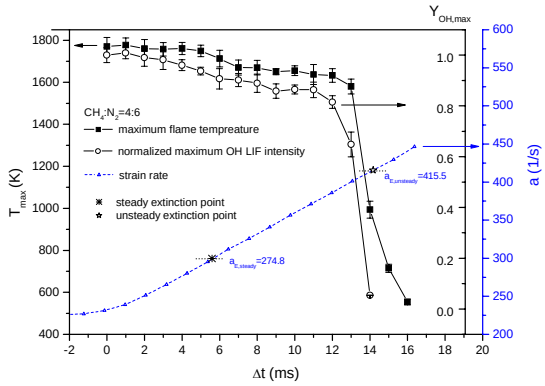

(a)

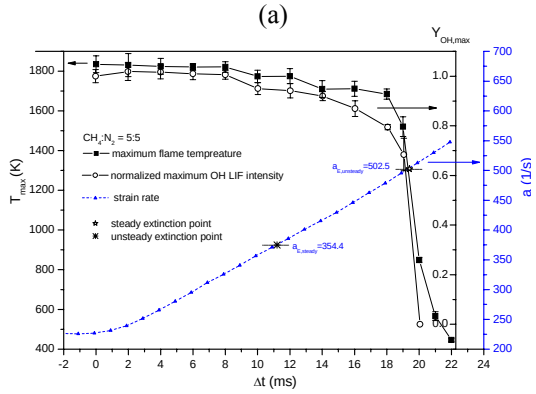

(b)

Fig. 6 Time-dependent maximum flame temperature, maximum relative OH intensity and extinction points of steady and unsteady flames ((a) CH_4:N_2= 4:6, (b) CH_4:N_2= 4:6)

with increasing the strain rate, and finally decreases rapidly near the extinction limit. The nearly constant values in the starting region result from the time lag of the convective-diffusive zone [7-10]. The lower bound of T_{max}, where the flame keeps its luminosity (1 ms before the extinction point) is roughly 1600 K. It is remarkable that the relative OH intensity rapidly decreases below the T_{max} = 1600 K. Near the extinction limits, the elapsed time for T_{max} decrease to the ambient temperature is 3-4 ms, i.e. comparable to the characteristic time of the flow (i.e. 1/strain rate)). The OH radical also has the residence time, but it is very short and less than 1 ms. These results imply that in contrast to the OH radical, the flame temperature depends on any unsteadiness in the flow near the extinction limit.

3.1.4. Unsteady behavior of a mixing layer. Figure 7a shows T_{max} of unsteady and quasi-steady cases with respect to instantaneous strain rate, and Figure 7b shows T_{max} with respect to the equivalent strain rate. The equivalent strain rate represents the delay in the convective-diffusive zone which means the retardation of the molecular diffusion with respect to the rapid change of instantaneous strain rate (convection). Considering the unsteady behavior of a mixing layer, it was reported that the temporal evolution of the equivalent strain rate $a(t)_{equivalent}$ from the instantaneous

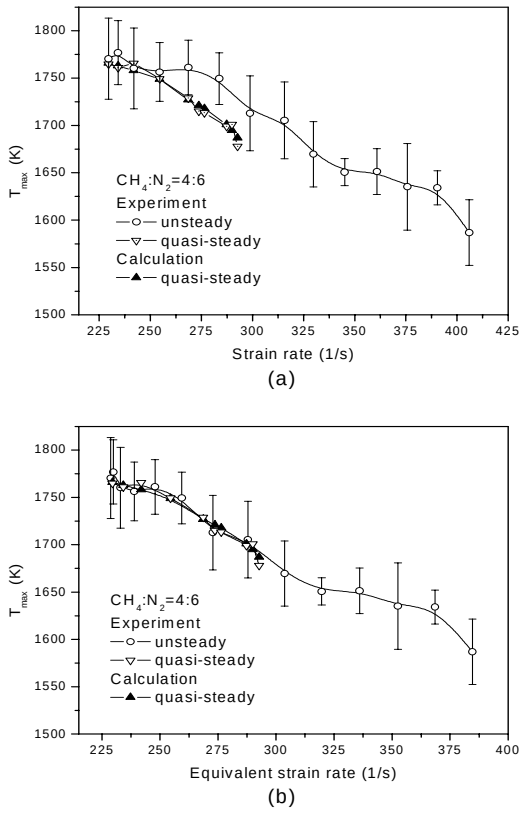

Fig. 7 (a) T_{max} versus instantaneous strain rate (b) T_{max} versus equivalent strain rate ($a_{initial}$ = 226.8 (1/s))

strain rate a(t) and initial strain rate a_0 [7]:

$$\frac{a_0}{a(t)_{equivalent}} = \frac{2a_0\int_0^t \exp[\int_0^{t'} 2a(t'')dt'']dt' + 1}{\exp[2\int_0^t a(t')dt']} \quad (3)$$

The equivalent strain rate has the same physical meaning as that for a scalar dissipation rate. In Fig. 7b, the unsteady extinction of the equivalent strain rate domain approximates the steady extinction in the starting region of the velocity change. This result means that the concept of the equivalent strain rate successfully estimates the time lag of the convective-diffusive zone. After subtracting the time lag of the convective-diffusive zone, the modified unsteady extinction limits approaches to the steady extinction limits, but remains larger than the steady extinction limits. Furthermore, even in the domain of the equivalent strain rate, the temperature of the unsteady flame still remains high above the steady extinction limit. All of these results verify that the diffusive-reactive zone behaves unsteadily near the extinction limit due to the chemical non-equilibrium states associated with unsteady flames.

4. Conclusion

To know why dynamic flames survive better than steady flames at a higher strain rate, we experimentally studied the unsteady behavior of a diffusion flame affected by velocity change. Detailed investigations of the unsteady extinction processes were accomplished. The unsteady extinction limits are much larger than the steady extinction limits. The time-dependent flame temperature and the relative OH LIF signal show the detailed characteristics of the unsteady extinction process. We obtained the T_{max} and Y_{OH} values of unsteady flames above the steady extinction limit and the T_{max} and $Y_{OH,max}$ values of the unsteady extinction limit. They are much lower than the corresponding values of the steady extinction limit.

To investigate the unsteady effect of the diffusive-reactive zone, we used the equivalent strain concept to subtract the time lag of the convective-diffusive zone. We found that the equivalent strain rate concept successfully estimates the time lag of the convective-diffusive zone. And we also found that the structure of the diffusive-reactive zone is affected by the flow unsteadiness and that unsteady behavior occurs in the diffusive-reactive zone near the extinction limit. Consequently, the unsteady response of the convective-diffusive zone and the diffusive-reactive zone should both be considered in order to explain the extension of the unsteady extinction limit. The former is dominant in the starting region of the velocity change and the latter is dominant near the extinction limit.

Acknowledgement

This work was supported by the Combustion Engineering Research Center (**CERC**) of KAIST.

References

[1] Williams, F. A., 2000, Prog. Energy Combust. Sci. 26, pp. 657-682
[2] Egolfopoulos, F. N. & Campbell, C. S., 1996, J. Fluid Mech. 318, pp.1-29
[3] Kistler et al. (1996) Proc. Combust. Inst. 26, pp.113-120
[4] Brown et al. (1998) Proc. Combust. Inst. 27, pp.703-710
[5] Lee et al. (2000) Proc. Combust. Inst. 28, pp.2079-2084
[6] Rolon, et al. (1995) Combust Flame 100, pp.422-429
[7] Santoro et al. (2000) Proc. Combust. Inst. 28, pp.2109-2116
[8] Kyritsis et al (2002) Proc. Combust. Inst. 29, pp.1679-1685
[9] Katta et al (2004) Combust Flame 137 (1-2), pp.198-221
[10] Oh et al. (2004) Combust Flame 138, pp.225-241
[11] Chelliah et al. (1990) Proc. Combust. Inst. 23, pp.503-511
[12] Namer I. & Schefer, R. W., 1985, Experiments in Fluids 3, pp.1-9
[13] Kee et al (2004) CHEMKIN Collection, Release 3.6, Reaction Design. Inc., San Diego, CA
[14] Smith et al. (2000) GRI-Mech 3.0.